# Hemodynamic dependence of myocardial oxygen consumption indexes

JOCHEN D. SCHIPKE, DANIEL BURKHOFF, DAVID A. KASS,
JOE ALEXANDER, JR., JOCHEN SCHAEFER, AND KIICHI SAGAWA†
*Division of Cardiology, The Johns Hopkins Hospital, Baltimore, Maryland 21205*

SCHIPKE, JOCHEN D., DANIEL BURKHOFF, DAVID A. KASS, JOE ALEXANDER, JR., JOCHEN SCHAEFER, AND KIICHI SAGAWA. *Hemodynamic dependence of myocardial oxygen consumption indexes.* Am. J. Physiol. 258 (Heart Circ. Physiol. 27): H1281–H1291, 1990.—We tested the afterload and contractile state dependency of three indexes of myocardial oxygen consumption ($M\dot{V}O_2$): total energy requirement ($E_t$), pressure work index (PWI), and pressure-volume area (PVA). $M\dot{V}O_2$ was measured in seven isolated canine hearts at four or five different end-diastolic volumes at each of three settings of afterload resistance and with the hearts contracting isovolumically. In several hearts, contractility was also varied by dobutamine infusion. Measured $M\dot{V}O_2$ ($M_{M\dot{V}O_2}$) was compared with values predicted ($P_{M\dot{V}O_2}$) by each index. There was always a high degree of correlation between $M_{M\dot{V}O_2}$ and $P_{M\dot{V}O_2}$ for each of the indexes. However, there was a large degree of variability in the coefficients of the $M_{M\dot{V}O_2}$-$P_{M\dot{V}O_2}$ relation from one heart to another. We also observed a statistically significant influence of both afterload and contractile state on the predictive power of each of the indexes. Thus each index that we tested had shortcomings in being able to predict $M\dot{V}O_2$ accurately over a wide range of hemodynamic conditions.

pressure-volume area; afterload; preload; contractility; heart rate; force-time integral

CENTRAL TO THE ANALYSIS of ventricular energetics is the measurement of myocardial oxygen consumption ($M\dot{V}O_2$) (8). This is because under aerobic conditions, $M\dot{V}O_2$ is closely linked to the utilization of ATP, which is the heart's principle source of chemical energy. Although the measurement of $M\dot{V}O_2$ is relatively simple in the isolated heart and in extensively instrumented animal preparations, it is difficult to measure $M\dot{V}O_2$ in the closed-chest animal or in patients. Therefore, several predictors of $M\dot{V}O_2$ have been proposed, which are based on more easily measured physiological signals. For the most part, each index attempts to quantitate total mechanical energy liberated by the heart, assuming that total mechanical work done by the ventricle correlates closely with $M\dot{V}O_2$.

There have been over 25 different indexes of $M\dot{V}O_2$ proposed over the past 70 years (1). In two earlier studies (1, 14), the ability of many of these indexes to predict measured $M\dot{V}O_2$ was compared under wide ranges of contractile states and loading conditions. However, no study has ever been done to specifically test whether the relation between measured and predicted $M\dot{V}O_2$ is influenced either by afterloading conditions or contractility. Furthermore, the interanimal variation in the ability of these indexes to predict $M\dot{V}O_2$ has been investigated in only one previous study (21). Despite this, it is claimed that some of these indexes are insensitive to load and contractility.

The purpose of the present study was to test and compare the predictive power of three different indexes of $M\dot{V}O_2$ in hearts contracting under a very wide range of hemodynamic conditions. We chose three indexes of $M\dot{V}O_2$ that have been investigated recently. The first of these was total energy requirement ($E_t$), which was proposed by Bretschneider (4). $E_t$ is the sum of five factors, each of which accounts for the energy required for a different process during a cardiac cycle. Next was the pressure-work index (PWI) proposed by Rooke and Feigl (14). This index is equal to the rate-pressure product plus two additional terms that account for external work and basal metabolism. Finally, the pressure-volume area (PVA) index developed by Suga et al. was chosen (21). This index has been proposed as a measure of the total mechanical energy liberated by the ventricle during a beat and has been shown to be linearly correlated to $M\dot{V}O_2$.

The predictive abilities of these indexes have never been compared with each other under comparable experimental conditions. Isolated hearts were used in this study because $M\dot{V}O_2$ can be measured accurately, the ventricles can be loaded in a physiological manner, and hemodynamic conditions can be defined precisely and varied over wide ranges. Measurements of $M\dot{V}O_2$, made at different afterload resistances and contractile states, were compared with values predicted by each of the three indexes.

## METHODS

*Surgical preparation.* A total of seven isolated canine hearts was studied. The procedures used to isolate and support a canine heart were similar to those described by Suga and Sagawa (19). A schematic of the preparation is presented in Fig. 1. A pair of mongrel dogs was anesthetized with pentobarbital sodium (30 mg/kg iv). The femoral arteries and veins of one dog (support dog) were cannulated and connected to a perfusion system that was used to supply oxygenated blood to the isolated heart. The chest of the second dog (donor dog) was opened

† Deceased 22 August 1989.

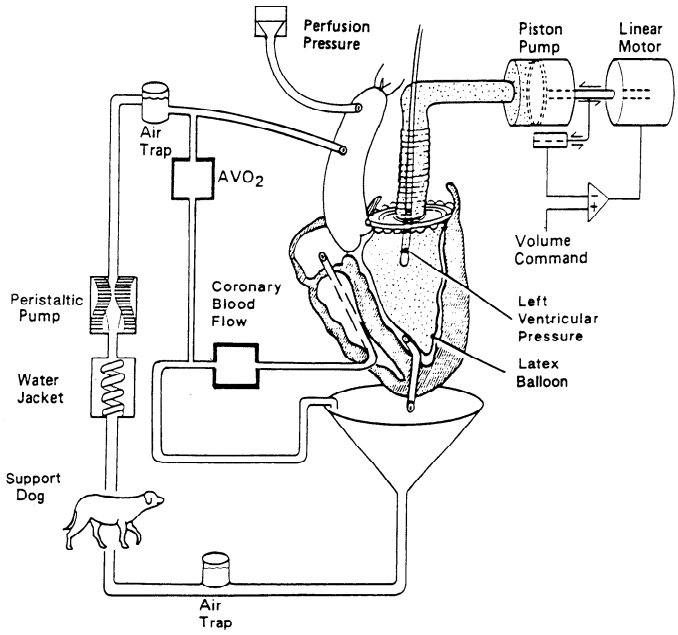


FIG. 1. Schematic diagram of isolated canine heart preparation. Coronary perfusion is maintained by a pump with blood from a support dog. A balloon is placed inside the left ventricle; balloon volume is controlled by a servo system. Physiological ejection and filling patterns are produced by interaction between heart and computer-simulated arterial and venous systems. Blood flow is measured by an electromagnetic flowmeter, and arteriovenous difference in oxygen content ($AVO_2$) is measured by spectrophotometric methods.

under mechanical respiration, and the heart was removed while metabolically supported by arterial flow from the support dog. The left atrium was opened, and all the chordae tendineae were freed from the mitral valve leaflets. A metal adapter that held the isolated heart to the ventricular volume servo-pump system (described below) was sutured to the mitral ring. A cannula, placed through the right ventricular apex and extending into the right atrium, was used to collect coronary venous blood flow. The right side of the heart was made airtight by ligation of superior and inferior vena cavae. When the surgical preparation was complete, a water-filled latex balloon, connected to the servo-pump system, was placed inside the left ventricular cavity. A micromanometer (Millar PC-380) placed inside the balloon was used to measure left ventricular pressure (LVP).

Coronary artery blood flow was regulated by a pulsatile pump that controlled the flow rate from the support dog. The flow of coronary venous blood draining into the right side of the heart was measured continuously by an electromagnetic flowmeter (Narco Bio Systems, RT-400). This flow represents total coronary blood flow (CBF) to both right and left ventricles except for the small amount of Thebesian flow draining directly into the left ventricle. The Thebesian portion of blood flow was neglected, since this has been shown to comprise a very small proportion of the total flow (12).

The difference in oxygen content between arterial and coronary venous blood ($AVO_2$) was measured continuously by absorption spectrophotometry [A-VOX Systems (15)]. The arterial pH, $PO_2$, and $PCO_2$ were measured periodically during each experiment to ensure nearly 100% $O_2$ saturation of the arterial blood during periods of data collection. Left ventricular oxygen consumption was calculated from the measurements of coronary blood flow and $AVO_2$ as described below.

The temperature of the perfusate was maintained at approximately 37°C by a heat exchanger. Pacing electrodes were sutured to atrial tissue to keep heart rate constant.

*Ventricular volume servo system.* Left ventricular volume (LVV) was controlled by a servo system, the design details and performance of which have been reported previously by Suga and Sagawa (20). As shown in Fig. 1, a linear motor controls the position of the piston within a rolling diaphragm cylinder. A latex balloon was secured to a tube connected to the outflow tract of the cylinder forming a closed system that was filled with water. A linear displacement transducer sensed the position of the piston, thus producing a signal proportional to balloon (and therefore ventricular) volume. This signal was used in a negative feedback loop for comparison with a volume command signal that represented the desired ventricular volume. The error signal resulting from this comparison was supplied to a power amplifier, which in turn drove the linear motor.

*Impedance loading system.* Physiological afterloading of the isolated left ventricles was accomplished by a computer-based system similar to that described in detail previously (22). Briefly, a digital computer was programmed with the differential equations of the three-element windkessel model of aortic input impedance. This model has been shown to provide a reasonable representation of the impedance spectra of real arterial systems (5) and consists of a characteristic impedance ($R_c$), arterial resistance ($R_a$), and arterial compliance ($C_a$). The computer digitizes the instantaneous LVP that it uses to calculate the appropriate instantaneous flow out of the ventricle; the flow signal is integrated, and the resulting signal is used as the volume command signal for the volume servo system. The values of the three windkessel parameters can be controlled from the computer keyboard, providing a means of altering afterload impedance.

Filling of the ventricle during diastole is accomplished by the computer that switches to a simple filling circuit consisting of a pressure source and filling resistance.

*Experimental protocol.* Experiments were performed on seven isolated hearts with an average left ventricular weight of 125 ± 9 g obtained from donor dogs with a mean body weight of 20.9 ± 0.8 kg. The hearts were paced at a constant rate (121 ± 6 beats/min) chosen to be approximately 10% above the spontaneous heart rate at the onset of the experiment. At a given setting of afterload we collected data at four or five different end-diastolic volumes. Over the course of the experiment, $R_a$ was set at 1.5, 3.0, and 6.0 mmHg·s·ml$^{-1}$, and in addition the heart was constrained to contract isovolumically. To avoid introduction of sequence-related bias into the data, we randomized the order in which the preload and afterload settings were varied. The final number of data points collected at each afterload from all seven hearts was 35 under isovolumic conditions, 30 with an $R_a$ of 6.0 mmHg·

$s \cdot ml^{-1}$, 33 with an $R_a$ of 3.0 $mmHg \cdot s \cdot ml^{-1}$, and 35 with an $R_a$ of 1.5 $mmHg \cdot s \cdot ml^{-1}$.

In four hearts, dobutamine (0.5 μg/min ic) was administered and heart rate simultaneously increased to 166 ± 6 beats/min with $R_a$ set at 3 $mmHg \cdot s \cdot ml^{-1}$. These data and the data obtained during control conditions defined above (with $R_a$ = 3.0 $mmHg \cdot s \cdot ml^{-1}$) were used to investigate the effect of the contractile state on the predictive power of the $M\dot{V}O_2$ indexes.

After any change in preload or afterload setting, or in heart rate and contractile state, data were recorded only after steady state was achieved in every signal monitored. This usually required about 4–5 min after a change.

At the end of each experiment, the weights of the right ventricular free wall and the left ventricle (LV) (left ventricular free wall plus ventricular septum) were measured.

*Data acquisition.* Left ventricular pressure, ventricular volume, arteriovenous difference in oxygen content, coronary venous blood flow, coronary arterial pressure, and arterial pressure of the support dog were recorded continuously (Gould, recorder 2800). All variables were stored on magnetic disk after digitizing at a sampling rate of 200 Hz for off-line analysis (DEC, LSI 11/23).

*Calculation of actual LV $M\dot{V}O_2$.* The $M\dot{V}O_2$ of the entire heart, i.e., of the LV plus the right ventricle (RV) (expressed in ml $O_2$/min), was equal to $CBF \cdot AVO_2$. However, we were interested in that portion of the oxygen consumed by the LV. To correct for this we assumed [as has been assumed by Suga et al. (16, 21)] that the RV was mechanically unloaded (i.e., not performing any external work) and consumed an amount of the total $M\dot{V}O_2$ determined when the LV was also mechanically unloaded, which was proportional to the RV weight, and that this amount was independent of the loading conditions on the LV. Accordingly, the RV $M\dot{V}O_2$ was estimated by multiplying total heart unloaded $M\dot{V}O_2$ (i.e., $M\dot{V}O_2$ when both LV and RV are mechanically unloaded) by the factor $W_{rv}/(W_{lv} + W_{rv})$, where $W_{lv}$ was the weight of the LV (LV free wall and septum combined), and $W_{rv}$ was the weight of the RV free wall. Total heart unloaded $M\dot{V}O_2$ was estimated as the $y$-axis intercept of the relation between measured total heart $M\dot{V}O_2$ vs. left ventricular pressure-volume area (see below for definition). RV $M\dot{V}O_2$ determined in this manner was considered to be independent of LV work load and was subtracted from whole heart $M\dot{V}O_2$ determined under the various work loads, and the result was defined as LV $M\dot{V}O_2$. A new estimate of RV $M\dot{V}O_2$ was made each time afterload was altered (as well as after administration of dobutamine) to account for fluctuations in base-line contractility that may have occurred during the time of the experiment, since fluctuations in contractility would influence RV $M\dot{V}O_2$ even in the absence of active RV work.

*Calculation of predicted $M\dot{V}O_2$.* The actual $M\dot{V}O_2$ calculated in the manner described above, was compared with each of the three predictions of $M\dot{V}O_2$ consumption. In the following paragraphs we will explain how $M\dot{V}O_2$ was predicted from measurements of ventricular pressure, volume, and other readily measured physiological parameters using the three different indexes.

Bretschneider's total myocardial energy demand, $E_t$ (4, 11), is given by

$$E_t = E_0 + E_1 + E_2 + E_3 + E_4 \quad (1)$$

where

$$E_0 = 7 \times 10^{-1} \text{ (ml } O_2 \cdot \text{min}^{-1} \cdot 100 \text{ g}^{-1})$$

$$E_1 = 3 \times 10^{-2} \cdot TS \cdot HR$$

$$E_2 = (1.4 \times 10^{-4} \cdot SBP^{1.5} \cdot TE \cdot HR)/(dP/dt_{max})^{1/3}$$

$$E_3 = 1.2 \times 10^{-5} \cdot (dP/dt_{max}) \cdot HR$$

$$E_4 = 8.0 \times 10^{-9} \cdot (dP/dt_{max})^{1.5} \cdot HR$$

and where HR is heart rate (beats/min); SBP is left ventricular peak systolic pressure (mmHg); $dP/dt_{max}$ is maximal rate of rise of left ventricular pressure (mmHg/s); TS is duration of electrical systole (s) that has been shown to be related to HR according to the following equation: $\sim 1/(1.08 + HR \cdot 2.24 \times 10^{-2})$; and TE is duration of ejection (s) that has been shown to be related to HR according to the following equation: $\sim 1/(2.7 + HR \cdot 2.32 \times 10^{-2})$.

All values needed in these equations can be obtained from the ventricular pressure tracing and from the heart rate. Because both TS and TE can be estimated directly from the heart rate, all elements of the equation can be evaluated under isovolumic conditions, and therefore $E_t$ should be able to predict $M\dot{V}O_2$ even under this extreme in loading conditions (personal communication, Bretschneider).

Rooke and Feigl (14) proposed PWI as a predictor of $M\dot{V}O_2$

$$M\dot{V}O_2 = 4.08 \times 10^{-4} \cdot (SBP \cdot HR) + 3.25 \times 10^{-4} \cdot (0.8 \cdot SBP + 0.2 \cdot DBP) \cdot HR \cdot SV/BW + 1.43 \quad (2)$$

where DBP is aortic diastolic blood pressure (mmHg); SV, stroke volume (ml); and BW is body wt (kg).

In our isolated heart preparation contracting against a computer-generated windkessel impedance, it was convenient to determine the systolic and diastolic pressures directly from the ventricular pressure tracings as follows. Systolic blood pressure was set equal to the peak left ventricular pressure. This is valid since, during ejection, proximal aortic and ventricular pressures are identical in the computer-generated afterload. Diastolic blood pressure was set equal to the ventricular pressure at the onset of ejection. This is valid since ejection begins at the point when ventricular pressure just slightly exceeds aortic pressure. Stroke volume was determined directly from the ventricular volume signal. It should be noted that under isovolumic conditions, the second term of *Eq. 2* becomes zero, and there is therefore no problem, in principle, in applying the equation to isovolumic conditions.

Suga et al. (21) proposed that $M\dot{V}O_2$ could be predicted from the PVA (in $mmHg \cdot ml \cdot 100\ g^{-1}$) according to the following equation

$$M\dot{V}O_2 = A \cdot HR \cdot PVA + B \cdot HR \cdot E_{es} + C \cdot HR \quad (3)$$

where $E_{es}$ is the slope of the end-systolic pressure-volume

relation ($mmHg \cdot ml^{-1} \cdot 100\ g$); $A$ is $1.8 \times 10^{-5}$ ml $O_2 \cdot mmHg^{-1} \cdot ml^{-1}$; $B$ is $2.4 \times 10^{-3}$ ml $O_2 \cdot beats^{-1} \cdot mmHg^{-1} \cdot ml \cdot 100\ g^{-1}$; and $C$ is $1.4 \times 10^{-2}$ ml $O_2 \cdot beats^{-1} \cdot 100\ g^{-1}$.

$E_{es}$, the slope of the end-systolic pressure-volume relationship (ESPVR), was calculated for each beat as indicated by Suga et al. (17, 21) by taking the slope of the straight line connecting the end-systolic pressure-volume point of the given beat to $V_0$ (volume axis intercept of the ESPVR)

$$E_{es} \equiv P_{es}/(V_{es} - V_0) \quad (4)$$

where $P_{es}$ and $V_{es}$ are end-systolic pressures and volumes, respectively, measured from each beat. $P_{es}$ and $V_{es}$ were defined as the point on the P-V loop at which the LVP-to-LVV ratio was maximum for a given beat. $V_0$, the volume at which end-systolic pressure is 0 mmHg, was estimated for each hemodynamic condition by linear extrapolation of the end-systolic pressure-volume data to the volume axis. In addition, the value of $E_{es}$ determined from *Eq. 4* was normalized to 100 g left ventricular mass.

Pressure-volume area was calculated by numerical (computer) integration, as outlined previously by Suga et al. (16) of the area bounded by the ESPVR, the systolic portion of the P-V loop, and the end-diastolic pressure-volume relation (which was presumed to be a straight line connecting the end-diastolic pressure-volume point to the $V_0$ point). PVA was also normalized to 100 g left ventricular weight (21).

*Statistics.* Linear regression analysis was applied to the $M_{M\dot{V}O_2}$-$P_{M\dot{V}O_2}$ data points obtained in each heart under each afterload condition to test load dependence of each predictor in individual hearts. To test whether there was any consistent influence of afterload between hearts we eliminated interanimal differences between hearts by a normalization procedure (see below), pooled data from each afterload, and, finally, applied analysis of covariance.

The normalization procedure was executed as follows. For each heart and for each index, the relation between measured and predicted $M\dot{V}O_2$ under isovolumic conditions was obtained by linear regression $P_{M\dot{V}O_2} = a\ M_{M\dot{V}O_2} + b$. When these $a$ and $b$ coefficients are applied, a linear transformation on the predicted $M\dot{V}O_2$ data was performed such that the resulting data for the isovolumic conditions now fell along the line of identity: $P_{M\dot{V}O_{2,norm}} = (P_{M\dot{V}O_2} - b)/a$. This same linear transformation was then applied to all the $P_{M\dot{V}O_2}$ data for that same heart under the three additional afterload conditions.

After the $P_{M\dot{V}O_2}$ data from each heart were transformed, data from all the hearts were pooled. The pooled regression between measured and transformed predicted $M\dot{V}O_2$ data for isovolumic conditions was the identity line and served as a standard for comparing the effect of afterload.

The influence of afterload was then assessed by an analysis of covariance (SYSTAT), coding afterload from low to high by a dummy variable (0–3). Tests for a significant interaction effect between afterload and the slope of the $M_{M\dot{V}O_2}$-$P_{M\dot{V}O_2}$ relationship were performed. If there was no interaction, then tests for a significant influence of afterload on the regression offset were made. If the above analysis revealed a significant interaction effect, paired comparisons between regressions (by covariance analysis) were performed using the Bonferoni correction for multiple comparisons.

The validity of the normalization procedure stemmed from the fact that for an individual heart, linear transformation of the data did not alter the statistical characteristics [i.e., standard estimated error (SEE) or correlation coefficient ($r^2$) value], nor did it alter the relative influence of afterload change. The process did help minimize differences between animals (which was its purpose), and thus reduced the disparity between individual dog regressions and regressions on the pooled data. This process then enabled the separate influence of afterload to be assessed from the total group data. The influence of contractility on the $M\dot{V}O_2$ predictors was performed in a similar manner to that described above for afterload.

## RESULTS

*Influence of afterload.* The contractile state, as quantified by $E_{es}$ and $V_0$, and $M\dot{V}O_2$ measured with the heart beating but mechanically unloaded ($M\dot{V}O_{2,0}$) from the seven hearts studied in this series are presented in Table 1. $E_{es}$ ranged from 3.69 to 7.57 $mmHg \cdot 100\ g \cdot ml^{-1}$ (mean 6.3), and $M\dot{V}O_{2,0}$ ranged from 0.0186 to 0.0455 ml $O_2 \cdot beat^{-1} \cdot 100\ g^{-1}$ (mean 0.0331). These ranges and average values are very similar to values obtained in isolated hearts by Suga and co-workers (16, 20). The average (± SD) ejection fraction measured from these hearts at an end-diastolic volume between 35 and 40 ml and an afterload resistance of 3 $mmHg \cdot s \cdot ml^{-1}$ was 37 ± 5%; under these conditions, the average end-systolic pressure was 90 ± 12 mmHg.

Results from a typical experiment are shown in Fig. 2. Each panel shows the relationship between $M_{M\dot{V}O_2}$ and $P_{M\dot{V}O_2}$ for a different predictor. The different symbols represent data obtained at different values of afterload resistance as indicated in the figure legend. The solid line in each panel of Fig. 2 represents the line of identity. In each case, there was a linear relationship between $M_{M\dot{V}O_2}$ and $P_{M\dot{V}O_2}$. Analysis of covariance applied to this single heart's data set revealed that the $M_{M\dot{V}O_2}$-$P_{M\dot{V}O_2}$ relationship was influenced by afterload ($P < 0.01$) in a few of the cases. However, despite the statistical signifi-

TABLE 1. *Base-line contractility and zero-work $O_2$ consumption for 7 hearts studied in first series of experiments*

| Expt. | $E_{es}$, $mmHg \cdot 100\ g \cdot ml^{-1}$ | $V_o$, ml | $M\dot{V}O_{2,0}$ | |
|---|---|---|---|---|
| | | | ml $O_2 \cdot beat^{-1} \cdot 100\ g^{-1}$ | ml $O_2 \cdot min^{-1} \cdot 100\ g^{-1}$ |
| 1 | 5.90 | 10.1 | 0.0415 | 4.98 |
| 2 | 7.33 | 13.6 | 0.0455 | 5.46 |
| 3 | 3.69 | 7.5 | 0.0265 | 3.34 |
| 4 | 6.12 | 7.0 | 0.0431 | 5.17 |
| 5 | 6.09 | 8.1 | 0.0218 | 2.18 |
| 6 | 7.39 | 6.0 | 0.0186 | 2.60 |
| 7 | 7.57 | 7.0 | 0.0346 | 3.46 |
| Means ± SD | 6.30±1.25 | 8.5±2.4 | 0.0331±0.0100 | 3.88±1.22 |

$E_{es}$, slope of end-systolic pressure; $V_o$, volume at which end-systolic pressure is 0 mmHg; $M\dot{V}O_{2,0}$, zero-work $O_2$ consumption. $M\dot{V}O_{2,0}$ is measured with heart beating but mechanically unloaded.

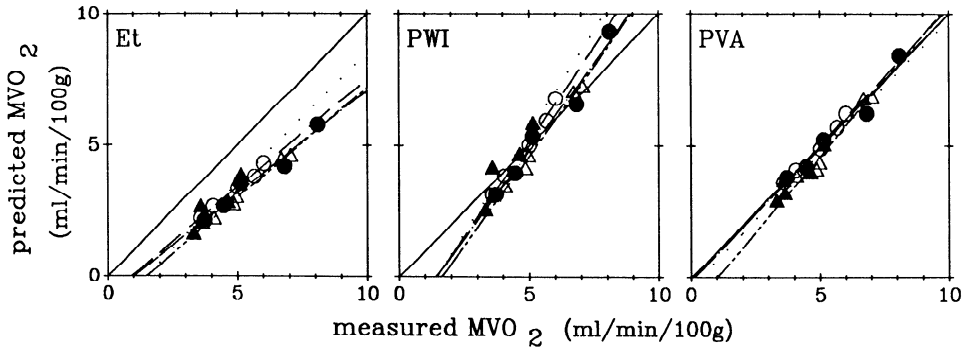


FIG. 2. Representative results from one ventricle showing the effect of changes in arterial resistance ($R_a$) on relationship between measured and predicted $M\dot{V}O_2$. $E_t$, total energy requirement; PWI, pressure work index; PVA, pressure-volume axis. Solid line in each panel is line of identity. Different symbols and lines indicate different values of $R_a$: open triangles, $R_a$ = 6.0; filled circles, $R_a$ = 3.0; open circles, $R_a$ = 1.5 mmHg·s$^{-1}$·ml$^{-1}$; filled triangles, isovolumic contractions.

cance of such differences in this heart, as seen in the graph, there is essentially no physiological significance to these differences. In this representative example, the $M_{M\dot{V}O_2}$-$P_{M\dot{V}O_2}$ relationship was different for each of the indexes. $E_t$ tended to underestimate actual $M\dot{V}O_2$ (on average for this heart, $P_{M\dot{V}O_2} = 0.87M_{M\dot{V}O_2} - 0.65$, $r^2 = 0.94$), PWI had a greater than unity slope but had a negative $y$-axis intercept ($P_{M\dot{V}O_2} = 1.27M_{M\dot{V}O_2} - 1.39$, $r^2 = 0.94$), and PVA provided an estimate very close to $M_{M\dot{V}O_2}$ ($P_{M\dot{V}O_2} = 1.05M_{M\dot{V}O_2} - 0.37$, $r^2 = 0.95$).

A summary of the data obtained from all seven ventricles is shown in Table 2. For each value of $R_a$, we present the average (± SD) slope ($m$), intercept ($b$), and correlation coefficient ($r^2$) of the $M_{M\dot{V}O_2}$-$P_{M\dot{V}O_2}$ relationship for each predictor. As shown, for a given predictor, there is relatively little variation in the mean coefficients from one afterload to another. However, it should be noted that the standard deviation about the mean is relatively large for the slope and intercept values in all cases. This indicates that from one heart to the next there is considerable variation in the $M_{M\dot{V}O_2}$-$P_{M\dot{V}O_2}$ relationship. There was relatively little variation in $r^2$, indicating that under all conditions the relationship was represented very well by a linear relation for all of the parameters at each of the loading conditions. The averaged and pooled data shown at the bottom of Table 2 will be discussed below (*Pooled data*).

TABLE 2. *Average effect (n = 7) of 4 different afterload resistances on the $M_{M\dot{V}O_2}$-$P_{M\dot{V}O_2}$ relations*

| $R_a$ | $E_t$ | PWI | PVA |
|---|---|---|---|
| 1.5 | | | |
| $m$ | 0.73±0.18 | 1.35±0.32 | 0.95±0.29 |
| $b$ | −0.61±0.87 | −2.41±1.80 | −0.15±2.14 |
| $r^2$ | 0.98±0.01 | 0.98±0.02 | 0.97±0.03 |
| 3.0 | | | |
| $m$ | 0.85±0.17 | 1.47±0.33 | 1.06±0.27 |
| $b$ | −0.79±0.80 | −2.10±1.40 | −0.01±1.85 |
| $r^2$ | 0.98±0.02 | 0.98±0.02 | 0.97±0.04 |
| 6.0 | | | |
| $m$ | 0.84±0.15 | 1.32±0.22 | 0.95±0.22 |
| $b$ | −1.15±0.80 | −2.04±1.39 | −0.03±2.25 |
| $r^2$ | 0.98±0.02 | 0.98±0.02 | 0.95±0.04 |
| Isovolumic | | | |
| $m$ | 0.87±0.20 | 1.22±0.43 | 0.88±0.39 |
| $b$ | −1.23±1.15 | −1.43±1.47 | 0.44±2.02 |
| $r^2$ | 0.95±0.06 | 0.92±0.10 | 0.88±0.12 |
| Average | | | |
| $m$ | 0.82 | 1.34 | 0.96 |
| $b$ | −0.95 | −2.00 | −0.06 |
| $r^2$ | 0.97 | 0.97 | 0.94 |
| Pooled | | | |
| $m$ | 0.51 | 0.84 | 0.56 |
| $b$ | 0.75 | 0.76 | 2.35 |
| $r^2$ | 0.72 | 0.72 | 0.55 |

Values are means ± SD; $n$ = 7 hearts. $R_a$, arterial resistance (in mmHg·s·ml$^{-1}$); $E_t$, Bretschneider's index for total energy demand; PWI, pressure-work index of Rooke and Feigl; PVA, pressure-volume area related index of Suga; $m$, slope of the linear regression line; $b$, intercept; $r^2$, coefficient of determinations.

A graphical representation of the statistical analysis used to test for afterload sensitivity of the PVA-based prediction of $M\dot{V}O_2$ is shown in Fig. 3. The pooled, linearly transformed data (see METHODS) obtained from all seven hearts under isovolumic conditions are shown in Fig. 3, top left panel. The normalization parameters were derived for each heart using the isovolumic data such that the relation between $M_{M\dot{V}O_2}$ and transformed $P_{M\dot{V}O_2}$ under isovolumic conditions would be the line of identity. This was accomplished, as shown, and furthermore this normalization procedure reduced interanimal variation of the relationship greatly. Also note that while the regression to the transformed data was the identity line, there was still significant scatter in the normalized data, which results from the variability in the original data.

The relationship between $M_{M\dot{V}O_2}$ and normalized $P_{M\dot{V}O_2}$

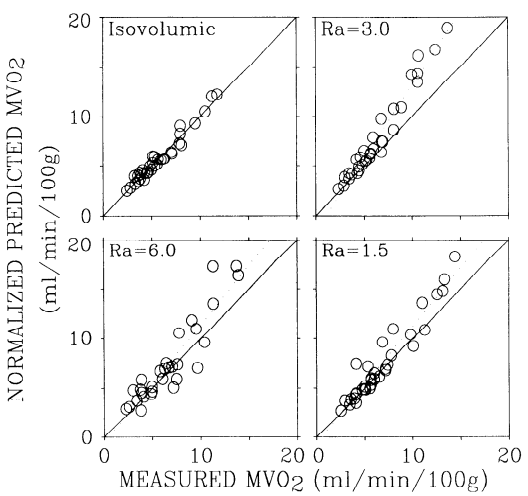


FIG. 3. Relations between measured $M\dot{V}O_2$ and normalized $M\dot{V}O_2$ predicted from PVA for 4 different afterloads ($R_a$) from 7 hearts studied. Normalization procedure, designed such that this relation would be line of identity under isovolumic conditions, reduced interanimal variations and revealed a consistent influence of afterload on the relation. See text and Table 3 for further explanation and results obtained from $E_t$- and PWI-based predictions of $M\dot{V}O_2$.

TABLE 3. *Summary of influence of afterload on the $M_{M\dot{V}O_2}$-normalized $P_{M\dot{V}O_2}$ relations for each index*

| Index | Isovolumic | | | $R_a$ = 1.5 | | | $R_a$ = 3.0 | | | $R_a$ = 6.0 | | |
|---|---|---|---|---|---|---|---|---|---|---|---|---|
| | $m$ | $b$ | $r^2$ | $m$ | $b$ | $r^2$ | $m$ | $b$ | $r^2$ | $m$ | $b$ | $r^2$ |
| PVA | 1.00 | 0.00 | 0.957 | 1.18 | −0.54 | 0.919 | 1.46*† | −1.51 | 0.958 | 1.20 | −0.58 | 0.845 |
| $E_t$ | 1.00 | 0.00 | 0.967 | 0.90 | 0.03 | 0.972 | 1.13† | −0.24 | 0.955 | 1.05 | −0.41 | 0.901 |
| PWI | 1.00 | 0.00 | 0.967 | 1.13 | −0.97 | 0.951 | 1.31*† | −1.08 | 0.924 | 1.13 | −0.73 | 0.925 |

Data were transformed such that relationship fell on the line of identity under isovolumic conditions. $M_{M\dot{V}O_2}$, measured myocardial $O_2$ consumption; $P_{M\dot{V}O_2}$, predicted myocardial $O_2$ consumption. * Regression line is significantly different from that obtained under isovolumic conditions ($P < 0.05$); † regression line is significantly different from that obtained with $R_a$ of 1.5 mmHg·s·ml$^{-1}$.

TABLE 4. *Average effect of contractility on relation between measured and predicted myocardial $O_2$ consumption for each of the indexes*

| | $E_{es}$ × 100 g | | $E_t$ | PWI | PVA |
|---|---|---|---|---|---|
| Control | 6.15±1.39 | $m$ | 0.79±0.17 | 1.37±0.27 | 1.06±0.27 |
| | | $b$ | −0.65±0.43 | −1.97±0.84 | 0.01±1.85 |
| | | $r^2$ | 0.98±0.01 | 0.99±0.01 | 0.97±0.04 |
| Dobutamine | 11.18±3.19 | $m$ | 0.80±0.06 | 1.49±0.21 | 0.47±0.43 |
| | | $b$ | −3.42±1.83 | −9.77±3.39 | 6.70±6.24 |
| | | $r^2$ | 0.95±0.02 | 0.90±0.10 | 0.85±0.15 |

Values are means ± SD; $n$ = 4 hearts. Afterload resistance set at 3.0 mmHg·s·ml$^{-1}$ for both conditions. Contractility enhanced by dobutamine (0.5 μg/min). Abbreviations as in Table 2. For further explanation see text.

determined under ejecting conditions for the other values of $R_a$ are shown in remaining panels Fig. 3. For each afterload, the regression line fell slightly above the line of identity. We used analysis of covariance to test whether any of these deviations from the isovolumic data were statistically significant, and the results showed that the relationship obtained with $R_a$ set at 3.0 mmHg·s·ml$^{-1}$ was significantly different than that obtained under isovolumic conditions ($P < 0.01$). Further analysis also showed that the relationships obtained at $R_a$ values of 3.0 and 1.5 mmHg·s·ml$^{-1}$ were significantly different from each other ($P < 0.01$).

A summary of the influence of afterload on the $M_{M\dot{V}O_2}$-normalized $P_{M\dot{V}O_2}$ relations for each of the three indexes is presented in Table 3. As shown, the relations obtained under isovolumic conditions and with an $R_a$ of 3.0 mmHg·s·ml$^{-1}$ were different for both PVA and PWI indexes, whereas the relations obtained with $R_a$ values of 3.0 and 1.5 mmHg·s·ml$^{-1}$ were different for all of the indexes.

*Influence of contractility.* The average results of the series of hearts in which we assessed the influence of dobutamine infusion on the predictive ability of each of the indexes are presented in Table 4. All of these experiments were performed under ejecting conditions with an $R_a$ value of 3.0 mmHg·s·ml$^{-1}$. The slope ($E_{es}$) was increased from an average of 6.15 to an average of 11.18 mmHg·100 g·ml$^{-1}$. There was a consistent near parallel rightward shift in the $M_{M\dot{V}O_2}$-$P_{M\dot{V}O_2}$ relations with increased contractility for both $E_t$- and PWI-based predictions of $M\dot{V}O_2$ (little change in mean slope, relatively big change in mean $y$-axis intercept) in each of the hearts. In contrast, the average $M_{M\dot{V}O_2}$-$P_{M\dot{V}O_2}$ relationship for the PVA-based prediction deviated significantly from that of base-line conditions, and there was a significant decrease in the linear correlation coefficient.

Of note, we originally studied five hearts in this protocol. However, there were three data points at the increased contractile state from one of these hearts for which PVA gave predictions of $M\dot{V}O_2$ that were far from the measured $M\dot{V}O_2$ ($P_{M\dot{V}O_2}/M_{M\dot{V}O_2} > 5$) and were excluded from analysis. These outliers are discussed further below. As a result of these outliers, there were useful data from only four of the hearts for analysis of the PVA index of $M\dot{V}O_2$. To ensure that the results of our comparison of indexes were based on the same set of data, analysis of PWI and $E_t$ predictors was based on data from the same four animals as were used for the PVA analysis. Therefore, the analysis presented above for the influence of contractility is based on data from only four of the five ventricles studied.

Results of the statistical analysis to test for a consistent influence of contractility on the predictive power of each of the indexes is summarized in Fig. 4 and Table 5. In each case, the data were transformed such that the $M_{M\dot{V}O_2}$-normalized $P_{M\dot{V}O_2}$ relation under control conditions would fall on the line of identity in each heart, and then the data were pooled. For both $E_t$ and PWI, analysis of covariance revealed a statistically significant decrease in offset value but not slope of the relation at enhanced

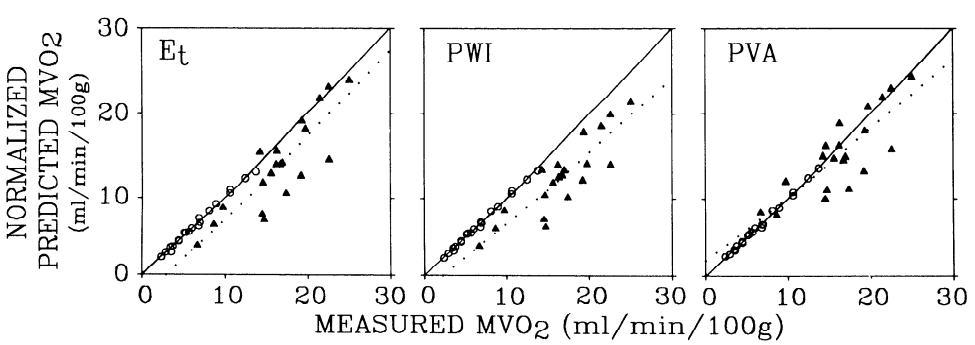


FIG. 4. Relationship between measured $M\dot{V}O_2$ and normalized predicted $M\dot{V}O_2$ for each of 3 indexes under control conditions (open circles) and after contractility was enhanced by dobutamine infusion (filled triangles) for 4 hearts studied. Solid lines, regression to control data; dotted lines, regression to dobutamine data. All measurements were made with hearts ejecting with an arterial resistance ($R_a$) value of 3.0 mmHg·s·ml$^{-1}$. Data were normalized so that relation was line of identity under control conditions. See Table 5 for quantitative summary of data.

TABLE 5. *Coefficients of relationship between $M_{M\dot{V}O_2}$ and normalized $P_{M\dot{V}O_2}$ measured at enhanced contractile state*

| Index | $m$ | $b$ | $r^2$ |
|---|---|---|---|
| $E_t$ | 1.02 | −2.95* | 0.74 |
| PWI | 0.87 | −1.95* | 0.77 |
| PVA | 0.82 | 1.93 | 0.66 |

Data were normalized such that the $M_{M\dot{V}O_2}$-normalized $P_{M\dot{V}O_2}$ relation was unity in the control contractile state in each heart, and then data from all hearts were pooled. * Elevation of the relation was significantly different from that measured under control contractile state by analysis of covariance ($P < 0.01$).

contractile states compared with control conditions. For PVA, however, there was no statistically significant deviation of the relation at the enhanced contractility. Note, however, that there was considerable scatter in the $M_{M\dot{V}O_2}$-normalized $P_{M\dot{V}O_2}$ relation measured under dobutamine as indicated by a relatively low value of $r^2$.

*Pooled data.* We present two ways of looking at the overall predictive power of the three indexes at the bottom of Table 2. First, we present the average coefficients of the $M_{M\dot{V}O_2}$-$P_{M\dot{V}O_2}$ relations obtained under the various afterloading conditions. Second, we pooled the raw data points from all hearts and all afterloading conditions and then applied linear regression analysis. As shown, there is a very large difference between the average regression coefficients and the regression on the pooled data. This indicates that the $M_{M\dot{V}O_2}$-$P_{M\dot{V}O_2}$ relations differ significantly from one heart to the next (a conclusion also supported by the large standard deviations of the regression parameters, as discussed above).

Figure 5 shows data pooled from all hearts, all afterload conditions, and all contractile states. In all, there are 153 individual determinations of $M\dot{V}O_2$ that comprised the data base. The results of linear regression analysis are presented in Table 6. Inclusion of the contractility data significantly broadened the range over which measured $M\dot{V}O_2$ varied. This had the effect of "improving" the $M_{M\dot{V}O_2}$-$P_{M\dot{V}O_2}$ relation for each of the indexes, in the sense that they became closer to the identity line and had higher $r^2$ values (compare the "pooled" results in Table 2 with the results of Table 6).

When analyzed in this manner, the PWI- and PVA-based predictions of $M\dot{V}O_2$ provided regression lines that were very close to the line of identity. $E_t$-based predictions consistently underestimated measured $M\dot{V}O_2$.

*Outliers.* When using the PVA-based predictor of $M\dot{V}O_2$, we encountered a few predictions that were very far from the measured values. This was the case for six pressure-volume loops (from a total of 159 predictions made) in all seven hearts studied. For these beats, $P_{M\dot{V}O_2}$ was more than five times greater than $M_{M\dot{V}O_2}$. Three of these points were obtained during the administration of dobutamine and at relatively low ventricular volumes (end-systolic volumes <20 ml). The other three points were obtained at the control contractile state but at the lowest preload setting investigated (end-systolic volumes ≤10 ml); two of these three points were obtained at an $R_a$ value of 3.0 mmHg·s·ml$^{-1}$, and the third was obtained during isovolumic conditions. Thus the common hemodynamic features of the beats in which this occurred were relatively low end-systolic ventricular volumes and/or high contractile states. Under such conditions $E_{es}$, as calculated from *Eq. 4*, is highly sensitive to the value of $V_0$. If it happens that the value of $V_0$ determined by linear regression from the group of end-systolic pressure-volume points is very similar to the lowest values of end-systolic volumes measured experimentally, then a very large (or even negative) $E_{es}$ can be obtained falsely from *Eq. 4*. This results in an erroneously large prediction of $M\dot{V}O_2$ (*Eq. 3*). Such outliers were excluded from the analysis presented above; furthermore, these same points were excluded from analyses involving PWI- and $E_t$-based predictions of $M\dot{V}O_2$ to ensure that all results obtained were from the same data base. There were no outliers encountered for the PWI- or $E_t$-based predictions of $M\dot{V}O_2$.

## DISCUSSION

We compared the hemodynamic dependencies of three predictors of $M\dot{V}O_2$. We chose indexes based on $E_t$, PWI, and PVA because they have each been shown, in different preparations, to provide excellent estimates of $M\dot{V}O_2$, they have received considerable attention in the literature previously, and the predictive power of the most recent of these, PVA, has never been compared with other indexes using the same data set. We did not explore the predictive power of the numerous other indexes because in previous reports PWI and $E_t$ have been shown to be superior to these other indexes (1, 14).

Our results show that in every heart the correlation between observed and predicted $M\dot{V}O_2$ was high for each of the indexes. There were statistically significant influences of afterload resistance on the $M_{M\dot{V}O_2}$-$P_{M\dot{V}O_2}$ relationships, indicating that changes in afterload can affect the predictive power of these indexes of $M\dot{V}O_2$. In some instances this effect was considerable (see Fig. 3 and Table 3). Changing contractility also created differences in the $M_{M\dot{V}O_2}$-$P_{M\dot{V}O_2}$ relationship, mostly manifested for

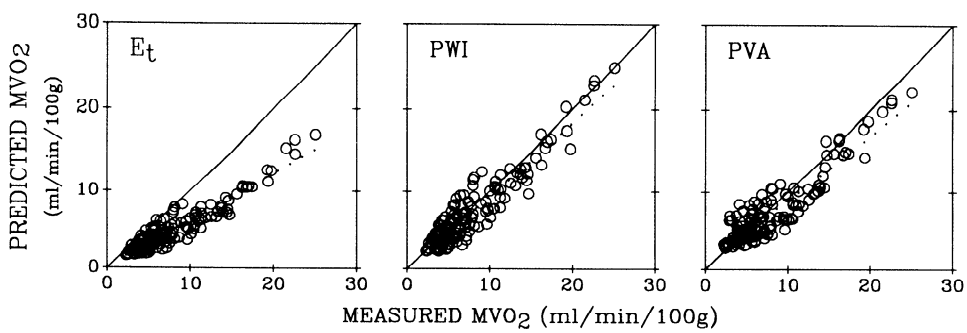


FIG. 5. Pooled data from all ventricles. Solid lines, lines of identity; dotted lines, lines of linear regression to data. See Table 6 for quantitative results.

TABLE 6. *Coefficients of $M_{M\dot{V}O_2}$-$P_{M\dot{V}O_2}$ relationship determined from data pooled from all hearts, all afterloads, and all contractile states for each of the predictors of $M\dot{V}O_2$*

| | $E_t$ | PWI | PVA |
|---|---|---|---|
| Slope | 0.60 | 0.90 | 0.80 |
| Intercept | 0.20 | 0.32 | 0.99 |
| $r^2$ | 0.88 | 0.87 | 0.83 |

Abbreviations as in Table 2.

the $E_t$ and PWI indexes as a rightward parallel shift. Our analysis also revealed that there was considerable variation among hearts in the relation between measured and predicted $M\dot{V}O_2$ for all of the predictors. As a result, the average regression coefficients of the $M_{M\dot{V}O_2}$-$P_{M\dot{V}O_2}$ relation for the individual hearts were quite different than those obtained when linear regression was applied to data pooled from all hearts.

In most of the previous evaluations of the predictive power of indexes of $M\dot{V}O_2$, the strategy has been to collect data from many hearts over a wide range of $M\dot{V}O_2$ values and apply linear regression analysis (or some other statistical analysis) to the pooled data (1–3, 21, 23). This would be similar to the results we present in Fig. 5 and Table 6, in which each predictor provided a highly correlated estimate of measured $M\dot{V}O_2$. Our results suggest that such an approach obscures heart-to-heart variations in the $M_{M\dot{V}O_2}$-$P_{M\dot{V}O_2}$ relationship. Suga et al. (21) also observed a heart-to-heart variation in the predictive power of $M\dot{V}O_2$ by PVA. Furthermore, Suga and colleagues (13, 16, 21) have repeatedly noted significant interanimal variations in the $M\dot{V}O_2$-PVA slope and intercept values, as well as some variations in the response of the $M\dot{V}O_2$-PVA relation to changes in inotropic state in the in situ dog heart (13). Burkhoff et al. (7) have also reported significant interanimal variation in the relation between contractile state and the intercept of the $M\dot{V}O_2$-PVA relation. Several explanations have been proposed to explain this interanimal variation, but the actual underlying reason has not been identified. It could be simply that there is significant biological variation in the quantitative relationships between work load and $M\dot{V}O_2$. Additionally, metabolic substrate utilization may vary from one experiment to another, and thus the proportion of ATP generated from breakdown of free fatty acid, glucose, acetate, pyruvate, etc, may differ; since the amount of ATP generated per mole oxygen consumed varies among these substrates, the $M_{M\dot{V}O_2}$-$P_{M\dot{V}O_2}$ relationship would be expected to vary. However, the degree of interanimal variation we observed is far greater than the known differences in the ratios between ATP production and oxygen consumptions.

We do not believe that methodological differences between our preparation and those used by other investigators contributed to our conclusions. $M\dot{V}O_2$ predicted from PVA were fairly accurate on the whole, at least when all the data are pooled (Table 6, Fig. 5). This should be expected, since our preparation is very similar to that used by Suga to obtain the parameters of the prediction equations. Despite our preparation being very different than that used by Rooke and Feigl (14), PWI provided as good a prediction of $M\dot{V}O_2$ as PVA (Table 6, Fig. 5). There was a consistent and significant underestimation of $M\dot{V}O_2$ by $E_t$ in all the hearts studied. The fact that $M\dot{V}O_2$ values predicted by the other two indexes were fairly accurate makes this underestimation real and considerable. Because the main effect was one of a reduced slope of the $M_{M\dot{V}O_2}$-$P_{M\dot{V}O_2}$ relationship without a significant offset, this problem could be easily compensated for by multiplying the equation for $E_t$ by a constant value to improve the value of the slope. We do not view this problem as a significant barrier to using $E_t$, since the correlation coefficient and the afterload dependency for $E_t$ were similar to those of the other predictors.

We encountered a problem using the PVA-based prediction of $M\dot{V}O_2$ at the high contractile state and at low volumes, which was not encountered in the other indexes. This appeared to be related to the high sensitivity of the estimation of $E_{es}$ from beats with low end-systolic volumes and/or high contractile states. As a result, there were six individual predictions (from a total of 159) that were outliers. This may have happened because we estimated $V_0$ by linear extrapolation of the ESPVR to the volume axis instead of actually measuring it as is done by Suga et al. (17, 21). This situation is not likely to occur under in situ conditions, since it is generally not possible to reduce end-systolic volume to the extent we can in the isolated heart.

It is interesting that the three indexes provide similar degrees of correlation between $M_{M\dot{V}O_2}$ and $P_{M\dot{V}O_2}$ despite their being based on seemingly unrelated measures of ventricular performance. Bretschneider's $E_t$ consists of five additive components, each considered to represent the energy consumption for a different process during the cardiac cycle: basal energy consumption, energy for electrophysiological processes, energy for maintenance of tension during systole, energy for tension development during isovolumic contraction, and energy for inactivation of the contractile system. With this approach $dP/dt_{max}$ is the index of contractility and therefore the only measurement needed for assessment of this index is high fidelity left ventricular pressure.

Rooke and Feigl's (14) PWI index consists of three additive components. The first of these is the systolic pressure-rate product which, by itself, has been shown to be a poor predictor of $M\dot{V}O_2$ (1–3, 14). The predictive power was improved when two more terms were added that accounted for left ventricular external work and for basal metabolism. The increased accuracy of PWI, however, is achieved with the additional requirement of having to measure stroke volume, which is not always possible under in situ conditions.

The PVA based index also consists of three components. One may be referred to as the PVA-dependent $M\dot{V}O_2$ ($A \cdot HR \cdot PVA$) and accounts for the amount of oxygen utilized for the total mechanical energy liberated by the heart during systole. The second component ($B \cdot HR \cdot E_{max}$) accounts for that portion of $M\dot{V}O_2$ that is utilized for excitation-contraction coupling that changes with contractile state. The third term is a constant and represents the fraction of $M\dot{V}O_2$ utilized for basal metabolism. Assessment of the PVA index requires the meas-

urement of end-systolic pressure and end-systolic volume at different preloads for determination of the end-systolic pressure-volume relation and for calculation of the pressure-volume area. Thus there is the need to measure instantaneous pressure and volume with reasonable accuracy, as well as perform some maneuver to estimate $V_0$ (e.g., vena caval occlusion).

One may argue that there is an intrinsic error in the equations from which $M\dot{V}O_2$ is predicted from PVA (*Eq. 3*). The equation, as written, predicts that $M\dot{V}O_2$ will become zero when the heart rate becomes zero. This is not the case in reality (e.g., with $K^+$ arrest), and neither the PWI nor the $E_t$ equation makes this incorrect prediction. The reason the formula takes the form that it does is probably because Suga et al. (18) have shown that within the range of heart rates that the isolated heart typically operates (between 100 and 180 beats/min), the relationship between $M\dot{V}O_2$ (expressed in ml $O_2$/beat) and PVA is independent of heart rate when $M\dot{V}O_2$ is expressed on a per beat basis. As a consequence, Suga's equation cannot apply under all circumstances. Equations of the form $P_{M\dot{V}O_2} = (A \cdot PVA + B \cdot E_{max})HR + C$ or $P_{M\dot{V}O_2} = (A \cdot PVA + B \cdot E_{max} + C)HR + D$ are likely to be more generally applicable. Unfortunately, there are no published data from which parameter values for these equations can be ascertained prospectively. The data of the present study cannot be used to generate these parameters values because we did not change heart rate in individual hearts.

Recently, Hasenfuss et al. (9) compared the relationships between measured $M\dot{V}O_2$ and several different correlates of $M\dot{V}O_2$, including PVA, PWI, $E_t$, and the stress-time integral (STI), in patients with dilated cardiomyopathy and with hemodynamic conditions varied by either nitroprusside or enoximone (a vasodilator and a positive inotropic agent). Hasenfuss et al. concluded that STI correlated best with $M\dot{V}O_2$. This is a surprising result in view of previous experimental findings regarding the STI and force-time integral (FTI), a similar measure to STI that is not normalized for cross-sectional area. Weber and Janicki (25) found that when contractility is increased in isolated canine hearts by dobutamine, $M\dot{V}O_2$ increases but FTI decreases. In a comparable study in papillary muscles, Hasenfuss et al. (10) showed that total heat liberation (a measure of chemical energy consumption) increases but STI decreases after addition of isoproterenol to the bathing solution. Most recently, Suga et al. (24) varied stroke volume while maintaining a constant PVA by decreasing afterload pressure and increasing end-diastolic volume. $M\dot{V}O_2$ remained constant (consistent with the constant PVA) but FTI decreased significantly. Thus these previous studies indicate that the relationship between $M\dot{V}O_2$ and FTI (or STI) is dependent on both afterload conditions and on contractility.

We examined our data to test the load and contractile state dependence on the correlation between $M\dot{V}O_2$ and FTI. We calculated FTI exactly as was done by Weber and Janicki (24) and Suga et al. (20); we also normalized FTI to 100 g LV weight to pool the data. We performed an identical statistical analysis on the $M\dot{V}O_2$-FTI relations as we did for PVA-, PWI-, and $E_t$-based predictions of $M\dot{V}O_2$. The results revealed significant interanimal variability in the $M\dot{V}O_2$-FTI relation. Furthermore, afterload resistance had a greater influence on the $M\dot{V}O_2$-FTI relation than on the three $M_{M\dot{V}O_2}$-$P_{M\dot{V}O_2}$ relations that were examined. Under ejecting conditions, there was a trend for the slope of the $M\dot{V}O_2$-FTI relation to increase as afterload resistance was decreased, consistent with the results of Suga et al. (20). Specifically, relations with $R_a$ values of 1.5 vs. 3.0 and 1.5 vs. 6.0 were significantly different ($P < 0.05$). The relation obtained under isovolumic conditions differed significantly from each of the ejecting conditions.

More impressive, however, was the influence of contractility on the $M\dot{V}O_2$-FTI relation. As reported by Weber and Janicki (25), enhancing contractility by dobutamine increased $M\dot{V}O_2$ but decreased FTI. This had the effect of shifting the $M\dot{V}O_2$-FTI relation upwards by an amount proportional to the change in contractility. On average $M\dot{V}O_{2(FTI=0)} = 0.82\ E_{es} + 0.62$ ($r = 0.65$, $P < 0.01$), where $M\dot{V}O_{2(FTI=0)}$ is the $M\dot{V}O_2$ intercept of the $M\dot{V}O_2$-FTI relation (ml $O_2 \cdot min^{-1} \cdot 100\ g^{-1}$) and $E_{es}$ is the index of contractility. The overall correlation between FTI and $M\dot{V}O_2$ is shown in Fig. 6 (see figure legend for details of regression coefficients). Pooling the data obtained under various afterloads at the control contractile state (open circles, regression line not shown) yielded a $r^2$ of 0.72 between $M\dot{V}O_2$ and FTI, which is as good as $E_t$ and PWI, and better than PVA-based predictions of $M\dot{V}O_2$ (see Pooled regressions in Table 2). However, when data obtained under enhanced contractile state were included in the regression (filled triangles, solid line), the $r^2$ decreased to 0.58, which is significantly worse than all of the other predictors of $M\dot{V}O_2$ (see Table 6 and Fig. 5). Thus consistent with results of previous studies, the correlation between FTI and $M\dot{V}O_2$ is not very good when contractility is not constant.

There are several factors to be considered when the conclusions of the present study are compared with that of Hasenfuss et al. (9). First, in their study PVA, obtained from different patients and under different contractile states created by enoximone, was correlated to $M\dot{V}O_2$

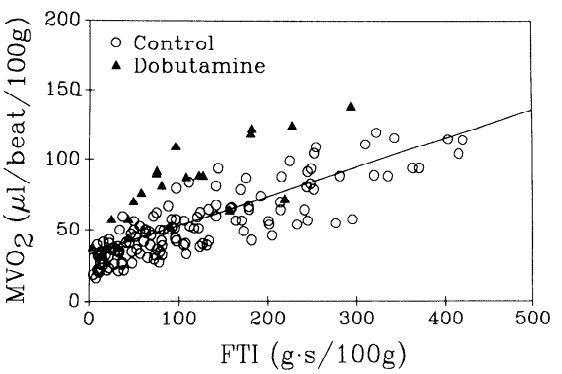


FIG. 6. Correlation between $M\dot{V}O_2$ and force-time integral (FTI). Data from all hearts, all afterload settings, but only control contractile state (open circles): $M\dot{V}O_2$ ($\mu l \cdot beats^{-1} \cdot 100\ g^{-1}$) = 0.204 FTI ($g \cdot s^{-1} \cdot 100\ g^{-1}$) + 29.0 ($r^2 = 0.72$). When data obtained under enhanced contractile state are included in regression (filled triangles, regression shown by solid line), $M\dot{V}O_2$ ($\mu l \cdot beats^{-1} \cdot 100\ g^{-1}$) = 0.207 FTI ($g \cdot s^{-1} \cdot 100\ g^{-1}$) + 32.7 ($r^2 = 0.58$). See text for further discussion.

regardless of contractility. This approach is contrary to the known contractility dependence of the $M\dot{V}O_2$-PVA relationship, which is accounted for in *Eq. 3* used in the present study (21). Additionally, $V_0$ was assumed to be zero for calculations of PVA. This assumption is almost certainly not reasonable (6) and could impact significantly on the conclusions, particularly when data are pooled from different patients with varying degrees of cardiac dilatation. Thus their analysis does not provide a fair or meaningful test of PVA. Furthermore, our results show that when using FTI (or STI) as a correlate of $M\dot{V}O_2$, the parameters of the relationship must be adjusted when contractility is changed. Another point to be considered is that Hasenfuss et al. (9) obtained only two data points in each patient and pooled data from many patients. Our results bring into question this approach, since there is significant interindividual variation in the correlation between $M\dot{V}O_2$ and each of the predictors examined.

*Conclusions.* The three predictors of $M\dot{V}O_2$ show a slight dependency on afterload conditions and a larger dependency on contractile state. All indexes showed differences between their predicting ability for single hearts and for pooled data. This observation has been reported previously for the PVA index but not for $E_t$ or PWI because analysis of single hearts was not performed in previous studies. This finding stemmed from the fact that there was significant interanimal variability in the relationship between measured and predicted $M\dot{V}O_2$ for each of the indexes. Since there was no striking differences in their predictive ability, the utility of an index in the clinical setting is related to the ease of its employment. In this regard, Bretschneider's (4) $E_t$ is probably the easiest to measure of the three indexes if high fidelity ventricular pressures are available, since it only requires measurement of ventricular pressure (and calculated $dP/dt_{max}$), whereas measurement of volumes (or stroke volume) are required for measurement of the other two indexes. Under situations when stroke volume can be estimated, PWI provides reasonable estimates of $M\dot{V}O_2$ from calculations that are simpler than those required for $E_t$. For all of the indexes, predicted $M\dot{V}O_2$ values must be interpreted with caution if changes in afterload conditions and especially if changes in the contractile state are likely to occur during the measurements. Comparison of predicted $M\dot{V}O_2$ between individuals may also be subject to considerable error. Our results indicate that, unlike PVA and PWI, $E_t$-based predictions of $M\dot{V}O_2$ consistently underestimated measured $M\dot{V}O_2$ (see averaged results of Table 2 and pooled results in Table 6), and this error could be corrected by simple scaling of the parameters of the prediction equation by a constant.

We thank Dr. H. J. Bretschneider for helpful suggestions. We thank Kenneth Rent for expert technical assistance during the experiments.

J. D. Schipke was supported in part by a postdoctoral fellowship grant from the American Heart Association, Maryland Affiliate, and by the German Research Foundation (DFG; Schi 201/1-1). This work was supported in part by National Heart, Lung, and Blood Institute Grant HL-18912.

Address for reprint requests: D. Burkhoff, Division of Cardiology, The Johns Hopkins Hospital, 600 N. Wolfe St., Carnegie 568, Baltimore, MD 21205.

Received 17 October 1988; accepted in final form 6 December 1989.

## REFERENCES

1. BALLER, D., H. J. BRETSCHNEIDER, AND G. HELLIGE. Validity of myocardial oxygen consumption parameters. *Clin. Cardiol.* 2: 317–327, 1979.
2. BALLER, D., H. J. BRETSCHNEIDER, AND G. HELLIGE. A critical look at currently used indirect indices of myocardial oxygen consumption. *Basic Res. Cardiol.* 76: 163–181, 1981.
3. BALLER, D., H. SCHENK, B. E. STRAUER, AND G. HELLIGE. Comparison of myocardial oxygen consumption indices in man. *Clin. Cardiol.* 3: 116–122, 1980.
4. BRETSCHNEIDER, H. J. Die hämodynamischen Determinanten des myokardialen Sauerstoffverbrauches. In: *Die therapeutischen Anwendung β-sympathikolytischer Stoffe*, edited by H. J. Dengler. Stuttgart: Schattauer, 1972, p. 45–60.
5. BURKHOFF, D., J. ALEXANDER, JR., AND J. SCHIPKE. Assessment of Windkessel as a model of aortic input impedance. *Am. J. Physiol.* 255 (*Heart Circ. Physiol.* 24): H742–H753, 1988.
6. BURKHOFF, D., J. T. FLAHERTY, D. T. YUE, A. HERSKOWITZ, R. Y. OIKAWA, S. SUGIURA, M. R. FRANZ, W. A. BAUMGARTNER, J. SCHAEFER, B. A. REITZ, AND K. SAGAWA. In vitro studies of isolated supported human hearts. *Heart Vessels* 4: 185–196, 1988.
7. BURKHOFF, D., D. T. YUE, R. Y. OIKAWA, M. R. FRANZ, J. SCHAEFER, AND K. SAGAWA. Influence of ventricular contractility on non-work-related myocardial oxygen consumption. *Heart Vessels* 3: 66–72, 1987.
8. GIBBS, C. L. Cardiac energetics. *Physiol. Rev.* 58: 174–254, 1978.
9. HASENFUSS, G., C. HOLUBARSCH, H. W. HEISS, T. MEINERTZ, T. BONZEL, U. WAIS, M. LEHMANN, AND H. JUST. Myocardial energetics in patients with dilated cardiomyopathy: influence of nitroprusside and enoximone. *Circulation* 80: 51–64, 1989.
10. HASENFUSS, G., C. HOLUBARSCH, H. JUST, E. BLANCHARD, L. A. MULIERI, AND N. R. ALPERT. Energetic aspects of inotropic interventions in rat myocardium. *Basic Res. Cardiol.* 82, *Suppl.* 2: 252–259, 1987.
11. HOEFT, A., H. KORB, D. BALLER, H. G. WOLPERS, G. HELLIGE, AND H. J. BRETSCHNEIDER. Quantification of ischemic stress during repeated coronary artery occlusion in the dog. A method for validating therapeutic effects. I. Estimation of $O_2$-debt and $O_2$-repayment. *Basic Res. Cardiol.* 79: 27–37, 1984.
12. MOIR, T. W., T. E. DRISCOL, AND R. W. ECKSTEIN. Thebesian drainage in the left heart of the dog. *Circ. Res.* 14: 245–249, 1963.
13. NOZAWA, T., Y. YASUMURA, S. FUTAKI, N. TANAKA, Y. IGARASHI, Y. GOTO, AND H. SUGA. Relation between oxygen consumption and pressure-volume area of in situ dog heart. *Am. J. Physiol.* 253 (*Heart Circ. Physiol.* 22): H31–H40, 1987.
14. ROOKE, G. A., AND E. O. FEIGL. Work as correlate of canine left ventricular oxygen consumption, and the problem of oxygen wasting. *Circ. Res.* 50: 273–286, 1982.
15. SHEPHERD, A. P., AND C. G. BURGAR. A solid-state arteriovenous oxygen difference analyzer for flowing whole blood. *Am. J. Physiol.* 232 (*Heart Circ. Physiol.* 1): H437–H440, 1977.
16. SUGA, H., Y. GOTO, T. NOZAWA, Y. YASUMARA, S. FUTAKI, AND N. TANAKA. Force-time integral decreases with ejection despite constant oxygen consumption and pressure-volume area in dog left ventricle. *Circ. Res.* 60: 797–803, 1987.
17. SUGA, H., R. HISANO, O. GOTO, O. YAMADA, AND Y. IGARASHI. Effect of positive inotropic agents on the relation between oxygen consumption and systolic pressure-volume area in canine left ventricle. *Circ. Res.* 53: 306–318, 1983.
18. SUGA, H., R. HISANO, S. HIRATA, T. HAYASHI, O. YAMADA, AND I. NINOMIYA. Heart rate-independent energetics and systolic pressure-volume area in dog heart. *Am. J. Physiol.* 244 (*Heart Circ. Physiol.* 13): H206–H214, 1983.
19. SUGA, H., AND K. SAGAWA. Instantaneous pressure-volume relationships and their ratio in the excised, supported canine left ventricle. *Circ. Res.* 35: 117–125, 1974.
20. SUGA, H., AND K. SAGAWA. End-diastolic and end-systolic ventricular volume clamper for isolated canine heart. *Am. J. Physiol.* 233 (*Heart Circ. Physiol.* 2): H718–H722, 1977.
21. SUGA, H., Y. YASUMURA, T. NOZAWA, S. FUTAKI, Y. IGARASHI,

AND Y. GOTO. Prospective prediction of $O_2$-consumption from pressure-volume area in dog hearts. *Am. J. Physiol.* 252 (*Heart Circ. Physiol.* 21): H1258–H1264, 1987.

22. SUNAGAWA, K., D. BURKHOFF, K. LIM, AND K. SAGAWA. Impedance loading servo pump system for excised canine ventricle. *Am. J. Physiol.* 243 (*Heart Circ. Physiol.* 12): H346–H350, 1982.
23. VINTEN-JOHANSEN, J., H. W. DUNCAN, J. G. FINKENBERG, M. C. HUME, J. M. ROBERTSON, R. J. BARNARD, AND G. D. BUCKBERG. Prediction of myocardial $O_2$ requirements by indirect studies. *Am. J. Physiol.* 243 (*Heart Circ. Physiol.* 12): H862–H868, 1982.
24. WEBER, K. T., AND J. S. JANICKI. Myocardial oxygen consumption: the role of wall force and shortening. *Am. J. Physiol.* 233 (*Heart Circ. Physiol.* 2): H421–H430, 1977.
25. WEBER, K. T., AND J. S. JANICKI. Interdependence of cardiac function, coronary flow, and oxygen extraction. *Am. J. Physiol.* 235 (*Heart Circ. Physiol.* 4): H784–H793, 1978.